IEEE Photonics Journal
An IEEE Photonics Society Publication

Demonstration of Distributed Strain Sensing With the Use of Stimulated Brillouin Scattering-Based Slow Light

Volume 3, Number 6, December 2011

Liang Wang, Student Member, IEEE
Chester Shu, Senior Member, IEEE

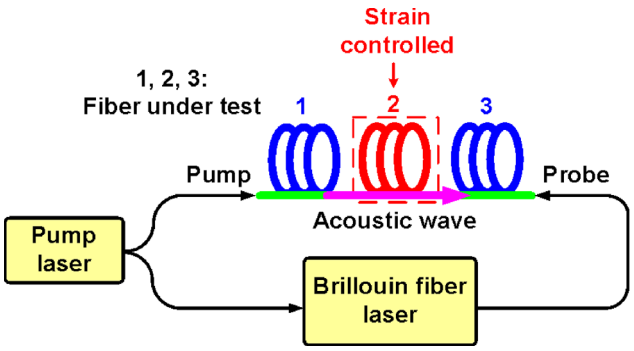

DOI: 10.1109/JPHOT.2011.2176112
1943-0655/$26.00 ©2011 IEEE

Demonstration of Distributed Strain Sensing With the Use of Stimulated Brillouin Scattering-Based Slow Light

Liang Wang, *Student Member, IEEE*, and Chester Shu, *Senior Member, IEEE*

Department of Electronic Engineering and Center for Advanced Research in Photonics, The Chinese University of Hong Kong, Shatin, Hong Kong

DOI: 10.1109/JPHOT.2011.2176112

Manuscript received October 4, 2011; revised November 7, 2011; accepted November 8, 2011. Date of publication November 16, 2011; date of current version December 6, 2011. Corresponding author: C. Shu (e-mail: ctshu@ee.cuhk.edu.hk).

Abstract: We demonstrate a distributed fiber-optic strain sensing scheme by measuring the delay time associated with stimulated Brillouin scattering-based slow light. The strain in any particular fiber section can be monitored by setting the counterpropagating pump and probe pulses to cross over in the region and recording the slow light delay. By scanning the crossover point along the sensing fiber, we have achieved distributed strain measurement. This scheme is simple to implement while offering a relatively high strain resolution of 13 $\mu\varepsilon$ and a spatial resolution of 15 m.

Index Terms: Distributed strain sensing, stimulated Brillouin scattering, slow light, delay time.

1. Introduction

The fiber-optic sensor is an excellent candidate for the monitoring of temperature and strain over long distances. The sensor offers the advantages of small size, immunity to electromagnetic interference, and survivability under harsh environments. Among the different types of sensors, Brillouin fiber sensors have attracted much research interest in the past two decades [1]–[10] and are now widely used in structural health monitoring. Characteristics of spontaneous and stimulated Brillouin scattering (SBS) are determined mostly by the material properties of the optical fiber. The amount of Brillouin frequency shift is related to the acoustic velocity and the refractive index, which are dependent on both the temperature and the strain of the fiber. Based on this principle, Brillouin fiber sensors have been demonstrated using the Brillouin optical time-domain reflectometer (BOTDR) configuration [1]. In addition, owing to the temperature and strain dependence of the frequency shift, the Brillouin gain or loss is also temperature and strain dependent, giving rise to Brillouin gain/loss-based sensors, such as the configurations for Brillouin optical time-domain analysis (BOTDA) [2]–[6] and Brillouin optical frequency-domain analysis (BOFDA) [7], [8]. The technique of Brillouin optical correlation-domain analysis (BOCDA) [9], [10] has also been used for Brillouin sensors to achieve centimetric resolution. These conventional Brillouin fiber sensors are promising for long-distance sensing with high resolution.

Apart from the applications in optical sensing, SBS can be used to achieve slow light in fibers [11]–[16]. Many applications have been found in optical communications, such as optical synchronization, optical multiplexing/demultiplexing, and optical equalization [16]. However, despite these applications, slow light is rarely associated with temperature or strain sensing. Recently, we have

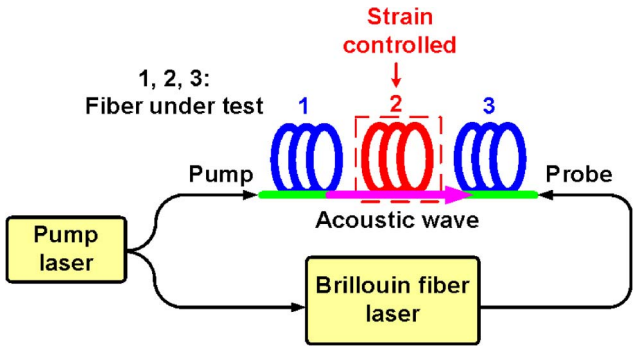

Fig. 1. Schematic illustration of the proposed distributed strain sensing scheme using SBS-based slow light.

demonstrated the feasibility of temperature sensing in fiber using SBS-based slow light [17]. The temperature of the sensing fiber was monitored by measuring the delay time of the probe pulse. A temperature resolution better than 1 °C was obtained. In addition to temperature sensing, by operating the pump in the pulsed mode and by combining the measurement results obtained at different positions, we have also realized distributed strain sensing along the whole fiber [18]. This approach can be potentially used in time-division multiplexing (TDM) sensing network [6]. The scheme offers an attractive means for temperature or strain monitoring without relying on optical beating to determine the narrow frequency shift using a radio-frequency spectrum analyzer. However, the work in [18] did not provide experimental details on the measurement error, the strain sensitivity, and the strain resolution. Here, we investigate the scheme more deeply by analyzing the above parameters and use three instead of two sections of fibers under test as in [18]. This is, to the best of our knowledge, the first reported work on distributed fiber-optic strain sensor exploiting SBS-based slow light. A strain resolution of 13 $\mu\varepsilon$ and a spatial resolution of 15 m are obtained.

2. Principle and Experimental Setup

Similar to temperature sensing using SBS-based slow light [17], the fundamental principle here is strain dependence of the Brillouin frequency shift in a fiber; hence, the delay time of an input probe pulse as a result of SBS-based slow light. The strain dependence of the delay time is governed by the following equation:

$$\Delta t = \Delta t_m \times \frac{1-\delta^2}{(1+\delta^2)^2} = \left(\frac{g_p L P_p}{\Gamma_B A_{eff}}\right) \frac{1-\delta^2}{(1+\delta^2)^2} \tag{1}$$

where

$$\delta = \frac{\Delta\Omega}{\Gamma_B/2} = \frac{2C_\varepsilon\ [\text{MHz}/\mu\varepsilon] \times (\xi - \xi_0)\ [\mu\varepsilon]}{(\Gamma_B/2\pi)\ [\text{MHz}]}. \tag{2}$$

Here, g_p is the Brillouin gain coefficient, L is the fiber length, P_p is the pump power, $\Gamma_B/2\pi$ is the gain bandwidth, A_{eff} is the fiber effective mode area, $\Delta\Omega$ is the frequency detuning of the probe from the Stokes wave in the fiber under test and $\delta = \Delta\Omega/(\Gamma_B/2)$ is its normalized value, $\Delta t_m = g_p L P_p/(\Gamma_B A_{eff})$ is the maximum delay time, C_ε is the strain coefficient of the Brillouin shift, ξ is the strain on the fiber under test, and ξ_0 is its initial value (generally set to zero microstrain).

Fig. 1 shows the working principle of our distributed strain sensing scheme. A continous wave (CW) pump laser is divided into two branches. The upper branch is used for the generation of pump pulses for SBS slow light, while the lower branch is applied as the pump for a Brillouin fiber laser. The fiber laser output is used to produce the probe pulse for SBS slow light. The probe pulse operates at the Stokes frequency of the fiber used in the Brillouin laser, which is of the same type of fiber under test. The arrangement provides automatic spectral alignment for wavelength transparent

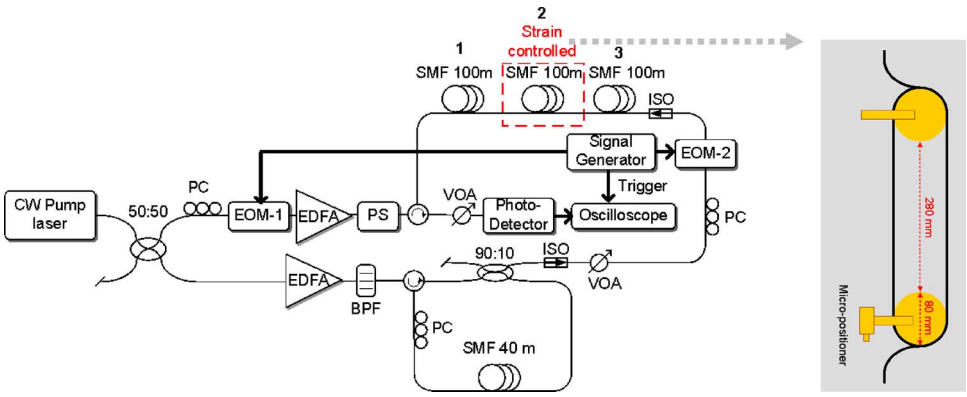

Fig. 2. Experimental setup for distributed strain sensing. Inset: schematic illustration of strain control in Section 2. EOM: electrooptic intensity modulator; EDFA: erbium-doped fiber amplifier; PC: polarization controller; VOA: variable optical attenuator; BPF: band pass filter; SMF: single mode fiber; ISO: isolator; PS: polarization scrambler.

slow light [14]. In our demonstration, we divide the fiber under test into three sections. The strain of the middle section (see Section 2) is varied and the other two sections (see Sections 1 and 3) are kept loose as the reference fibers. The slow light effect is introduced inside the fiber under test. The duration and the length of interaction are determined by the widths of the counterpropagating pump and probe pulses. If the two pulses meet at Sections 1 or 3, the probe will experience the maximum delay because its frequency is automatically aligned to that of the Stokes wave in the sections. If the two pulses meet at Section 2, the probe will experience a delay that is dependent on the strain in the fiber. The underlying principle is that the Brillouin frequency shift in Section 2; hence, the SBS gain of the probe is determined by the strain in the fiber. By controlling the relative delay between the pump and probe pulses, the crossover point can be set at any arbitrary position. Through measuring the SBS delay for the cases of different crossover points, the strain distribution along the whole sensing fiber can be retrieved.

The experimental setup is shown in Fig. 2. A CW pump laser at 1550 nm is split into two branches. The upper branch is modulated by an electrooptic intensity modulator (EOM-1) to provide a 100-ns rectangular pump pulse. After an amplification, the pump pulse passes through a polarization scrambler to minimize the polarization-induced noise [19] which will otherwise result in fluctuations of the SBS probe delay and thus the accuracy of our scheme. The lower branch is amplified to pump a Brillouin fiber laser constructed with 40-m single mode fiber (SMF). The laser output is intensity-modulated by EOM-2 to produce a 50-ns probe pulse. The pump and probe pulses are synchronized at 50 kHz repetition frequency and their relative delay can be controlled by the signal generator. The relative delay determines the crossover point of the two counter-propagating pulses in the fiber under test, where SBS slow light is introduced. The probe pulse is then measured by a photodetector and displayed on an oscilloscope for the determination of SBS slow light delay. The compositions of the fiber under test are three sections of 100-m SMFs. During the experiment, variable strain is applied to the middle 100-m SMF section wound around a couple of plastic drums with a diameter of 80 mm. One of the drums is supported by a micropositioner of which the movement controls the strain value. The other two sections of 100-m SMF are free from strain, serving as reference fibers.

3. Results and Discussions

Fig. 3 plots the delayed probe pulses when the crossover of the pump and probe occurs at different positions along the fiber: length $L = 50$ m, 150 m, and 250 m, corresponding to crossover at Sections 1–3, respectively. The red, green, and blue curves in Fig. 3(a) show that the probe pulses experience almost the same amount of delay. The result is expected as the three sections of the fiber under test are all free from strain. The achievable maximum delay time is $\sim$14.0 ns. Next, we

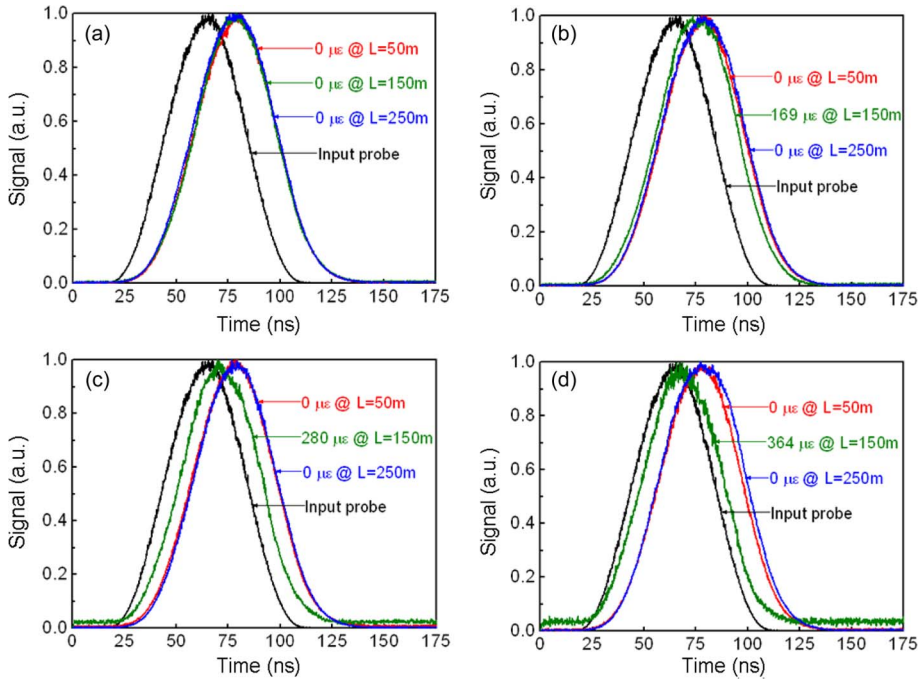

Fig. 3. (a)–(d) Measured output probe pulses for three different crossover (sensing) points at Section 1 ($L = 50$ m), Section 2 ($L = 150$ m), and Section 3 ($L = 250$ m) when the strain in Section 2 is maintained at (a) 0, (b) 169, (c) 280, and (d) 364 $\mu\varepsilon$.

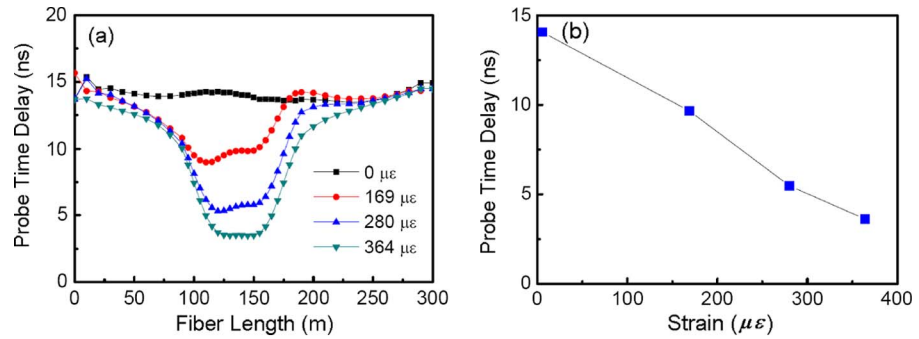

Fig. 4. (a) Delay time of the probe pulse when the pump and probe pulses cross at different positions along the sensing fiber. The strains in Section 2 are set at 0, 169, 280, and 364 $\mu\varepsilon$, respectively. (b) Average values of the delay times at Section 2 as derived from the data in (a).

adjust the strain in Section 2 to 169, 280, and 364 $\mu\varepsilon$, respectively, and repeat the measurement. The delayed probe pulses are shown in Figs. 3(b)–(d). The SBS delay is almost unchanged ($\sim$14.0 ns, shown as the red and blue curves) for the cases when the crossover occurs at Sections 1 or 3. However, the delay is reduced when the crossover is at Section 2 as the strain is increased. The results are displayed as the green curves. In Fig. 3, a slight distortion of pulses is observed and is attributed mainly to the limited SBS gain bandwidth. The signal-to-noise ratio (SNR) can be further improved by using the averaging function in the oscilloscope. Note that if there are strains applied on all the three sections at the same time, the red and blue curves in Fig. 3 will exhibit delays shorter than 14.0 ns. The amount of delays will depend on the exact strain values.

For distributed strain sensing, we also measure the probe delay time at other crossover positions. For each set of measured data along the sensing fiber, an average was taken over every five measurement positions for three times in order to minimize the effect of noise. Fig. 4(a) shows the

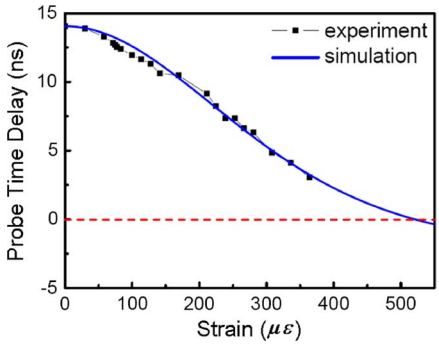

Fig. 5. Experimental data (dark squares) and simulated curve on the probe delay time versus the strain at Section 2 when the pump and probe crossover is fixed at $L = 150$ m.

delay time of the probe pulse when Section 2 is maintained at four different strains. One can clearly distinguish the delay time at Section 2 from those at Sections 1 and 3. The average values (14.06, 9.66, 5.48, and 3.62 ns) of the delay times at Section 2 versus the four strain levels are shown in Fig. 4(b). The spatial resolution of our sensing technique is the overlapping distance of the pump and probe pulses along the fiber where the interaction takes place [20]. The resolution is $\sim$15 m, as determined from the product of the group velocity and the average of the pump and probe pulse widths. This is only a conservative estimation since the calculated distance includes the whole duration of partial and complete overlapping of pulses. Certainly, the spatial resolution can be improved by using shorter pulses. However, a shorter probe pulse will imply a broader spectral width, resulting in more pulse distortion due to the limited SBS gain bandwidth. The width of the shortest pulse that can be delayed is $\sim$20 ns under the intrinsic SBS gain bandwidth. The pulse distortion affects the accuracy of our scheme and hence limits further improvement of the spatial resolution.

In a subsequent experiment we investigate the measurement error, the strain sensitivity, and the strain resolution. We apply different strains on Section 2 and record the probe delay versus the strain when the crossover point is fixed at $L = 150$ m, the center position of Section 2. The experimental data are shown as the dark squares in Fig. 5. The strain sensitivity of the delay is $\sim$0.03 ns/$\mu\varepsilon$ The blue curve in Fig. 5 shows the simulated relationship between the probe delay and the strain at Section 2. The simulation is based on (1) and (2) using strain coefficient $C_\varepsilon = 0.048$ MHz/$\mu\varepsilon$ [21], initial strain $\xi_0 = 0$ $\mu\varepsilon$, SBS gain bandwidth $\Gamma_B/2\pi = 50$ MHz [17], and maximum delay time $\Delta t_m = 14.06$ ns (obtained from our experiment). Limited by the SBS gain bandwidth, the maximum strain sensing value is $\sim$520 $\mu\varepsilon$ as the delay time will become negative, owing to fast light beyond this strain value. Similar to [17], the measurement error can be approximated by the root-mean-square deviations between the experimental data and the simulated result. The error is found to be 0.40 ns. Like most of the approaches [3], [6], [9], [10] used in calculating strain/temperature resolution, we take the ratio of the measurement error and the strain sensitivity to obtain the strain resolution. The result is $\sim$13 $\mu\varepsilon$. The resolution can be enhanced by increasing the strain sensitivity or reducing the measurement error. To improve the strain sensitivity, one can increase the pump power to enhance the SBS gain and thus the time delay of the probe pulse. To reduce the measurement error, several factors should be considered. The error can originate from pump power fluctuations, polarization-induced pulse distortion [19], and intensity noise transferred from the instability of the Brillouin fiber laser [14]. These factors can result in fluctuations of the probe pulse delay and hence inaccuracy of the measurement. Therefore, a laser with steady output power, a polarization scrambler, and a stable Brillouin fiber laser cavity should be employed together with the averaging function of the oscilloscope. In addition, probe pulse distortion due to the limited SBS gain bandwidth will cause difficulties in determining the delay time, hence contributing to measurement error. Wider probe pulse will experience less distortion to improve the accuracy and strain resolution. However, the spatial resolution will be reduced. A tradeoff should be adopted between strain resolution and spatial resolution according to practical considerations.

It is worth mentioning that the measurable range of strain values can be enlarged by slightly modifying the configuration. The pump can be served by a wavelength-tunable laser while the probe is served by a wavelength-fixed laser instead of the Brillouin fiber laser. By applying pump pulses at different wavelengths, each defining a unique measurable range of strain in our setup, the total sensing range can be enlarged. Alternatively, the setup shown in Fig. 2 can be directly applied to increase the measurable range of strain values simply by maintaining the fiber in the Brillouin laser at different strain levels. Each selected strain sets the reference for the starting point of a strain sensing range.

The maximum sensing distance in our scheme is limited by fiber attenuation. For a long distance, the attenuation should be considered since it affects the pump power level and, hence, the probe pulse delay. The accuracy in strain monitoring will be affected. To extend the maximum sensing distance, in-line Raman amplifiers [4] can be adopted to compensate for the optical loss.

4. Conclusion

By measuring the delay time of a probe pulse for the cases of different pump-probe crossover positions along the fiber, a distributed strain sensing scheme has been demonstrated using SBS-based slow light. Three sections of fibers are used in the setup to demonstrate our scheme. The sensing scheme has been analyzed by a combination of experiment and simulation. We achieve a spatial resolution of 15 m and a strain resolution of 13 $\mu\varepsilon$. Our scheme is simple to realize and is practical for accurate monitoring of the strain.

References

[1] S. M. Maughan, H. H. Kee, and T. P. Newson, "57-km single-ended spontaneous Brillouin-based distributed fiber temperature sensor using microwave coherent detection," *Opt. Lett.*, vol. 26, no. 6, pp. 331–333, Mar. 2001.
[2] X. Bao, D. J. Webb, and D. Jackson, "32-km distributed temperature sensor based on Brillouin loss in an optical fiber," *Opt. Lett.*, vol. 18, no. 18, pp. 1561–1563, Sep. 1993.
[3] H. Liang, W. Li, N. Linze, L. Chen, and X. Bao, "High-resolution DPP-BOTDA over 50 km LEAF using return-to-zero coded pulses," *Opt. Lett.*, vol. 35, no. 10, pp. 1503–1505, May 2010.
[4] F. R. Barrios, S. M. López, A. C. Sanz, P. Corredera, J. D. A. Castañón, L. Thévenaz, and M. G. Herráez, "Distributed Brillouin fiber sensor assisted by first-order Raman amplification," *J. Lightw. Technol.*, vol. 28, no. 15, pp. 2162–2172, Aug. 2010.
[5] S. M. Lopez, M. A. Camas, F. Rodriguez, P. Corredera, J. D. A. Castañón, L. Thévenaz, and M. G. Herráez, "Brillouin optical time-domain analysis assisted by second-order Raman amplification," *Opt. Express*, vol. 18, no. 18, pp. 18 769–18 778, Aug. 2010.
[6] Y. Dong, L. Chen, and X. Bao, "Time-division multiplexing-based BOTDA over 100 km sensing length," *Opt. Lett.*, vol. 36, no. 2, pp. 277–279, Jan. 2011.
[7] R. Bernini, A. Minardo, and L. Zeni, "Stimulated Brillouin scattering frequency-domain analysis in a single-mode optical fiber for distributed sensing," *Opt. Lett.*, vol. 29, no. 17, pp. 331–333, Sep. 2004.
[8] A. Minardo, R. Bernini, and L. Zeni, "Brillouin optical frequency-domain single-ended distributed fiber sensor," *IEEE Sensors J.*, vol. 9, no. 3, pp. 221–222, Mar. 2009.
[9] K. Hotate and M. Tanaka, "Distributed fiber Brillouin strain sensing with 1-cm spatial resolution by correlation-based continuous-wave technique," *IEEE Photon. Technol. Lett.*, vol. 14, no. 2, pp. 179–181, Feb. 2002.
[10] M. Belal and T. P. Newson, "Enhanced performance of a temperature-compensated submeter spatial resolution distributed strain sensor," *IEEE Photon. Technol. Lett.*, vol. 22, no. 23, pp. 1705–1707, Dec. 2010.
[11] M. G. Herráez, K. Y. Song, and L. Thévenaz, "Optically controlled slow and fast light in optical fibers using stimulated Brillouin scattering," *Appl. Phys. Lett.*, vol. 87, no. 8, p. 081113, Aug. 2005.
[12] M. G. Herráez, K. Y. Song, and L. Thévenaz, "Arbitrary-bandwidth Brillouin slow light in optical fibers," *Opt. Express*, vol. 14, no. 4, pp. 1395–1400, Feb. 2006.
[13] Y. Okawachi, M. S. Bigelow, J. E. Sharping, Z. Zhu, A. Schweinsberg, D. J. Gauthier, R. W. Boyd, and A. L. Gaeta, "Tunable all-optical delays via Brillouin slow light in an optical fiber," *Phys. Rev. Lett.*, vol. 94, no. 15, p. 153902, Apr. 2005.
[14] A. Cheng, M. P. Fok, and C. Shu, "Wavelength-transparent, stimulated-Brillouin-scattering slow light using cross-gain-modulation-based wavelength converter and Brillouin fiber laser," *Opt. Lett.*, vol. 33, no. 22, pp. 2596–2598, Nov. 2008.
[15] S. Chin and L. Thévenaz, "Optimized shaping of isolated pulses in Brillouin fiber slow-light systems," *Opt. Lett.*, vol. 34, no. 6, pp. 707–709, Mar. 2009.
[16] A. E. Willner, B. Zhang, L. Zhang, L. Yan, and I. Fazal, "Optical signal processing using tunable delay elements based on slow light," *IEEE J. Sel. Topics Quantum Electron.*, vol. 14, no. 3, pp. 691–705, May 2008.
[17] L. Wang, B. Zhou, C. Shu, and S. He, "Stimulated Brillouin scattering slow-light-based fiber-optic temperature sensor," *Opt. Lett.*, vol. 36, no. 3, pp. 427–429, Feb. 2011.

[18] L. Wang and C. Shu, "Distributed fiber strain sensor using stimulated Brillouin scattering based slow light," presented at the IEEE Photonics Conf., Arlington, VA, Oct. 2011, Paper ThEE 4.
[19] A. Zadok, S. Chin, L. Thévenaz, E. Zilka, A. Eyal, and M. Tur, "Polarization-induced distortion in stimulated Brillouin scattering slow-light systems," *Opt. Lett.*, vol. 34, no. 16, pp. 2530–2532, Aug. 2009.
[20] M. Nikles, L. Thévenaz, and P. A. Robert, "Simple distributed fiber sensor based on Brillouin gain spectrum analysis," *Opt. Lett.*, vol. 21, no. 10, pp. 758–760, Aug. 1996.
[21] M. Alahbabi, Y. T. Cho, and T. P. Newson, "Comparison of the methods for discriminating temperature and strain in spontaneous Brillouin-based distributed sensors," *Opt. Lett.*, vol. 29, no. 1, pp. 26–28, Jan. 2004.